Investigation of Workforce Dynamical Behaviour from a Phase Plane Perspective

Timo Lahteenmaa-Swerdlyk and François-Alex Bourque
Centre for Operational Research and Analysis, Development Research and Defence Canada,

Keywords: Differential Equation, Mentee, Mentor, Mentoring, Population Dynamics, Population Model.

Abstract: The purpose of this work was to investigate the population dynamics of on-the-job training. The ratio of mentees to mentors was considered, and its effect on overwhelming (saturating) the training system was analysed when undergoing a growth phase between two healthy states. This analysis was completed by analytically solving a simplified continuous model of the problem with constant input parameters. The model was investigated through a phase-plane interpretation, or the mentee versus mentor population as the system evolves. The key input parameter of the analysis was the saturation limit: the ratio of mentees to mentors above which the system becomes saturated. This value can be modified by adjusting various factors such as the quality, quantity, and/or the delivery method of the training. Of special interest was the time for the system to evolve as the saturation limit was varied. It was discovered that the system behaviour can fall into three categories based on its value. If the saturation limit is very low, the system will remain saturated and never reach a steady state. If the threshold is very high, the system will remain unsaturated (healthy) and reach steady state at inputted target populations, albeit in a relatively slow timeframe. Finally, for a particular middle range of values, the system will reach steady state at inputted target populations in an optimal time by crossing into and out of saturation. Therefore, finding the optimal values for the input parameters will depend on a compromise between reaching the target state quickly and not exceeding the target population levels, which will depend on the priorities of the organization. Given that any occupation with on-the-job training could experience such effects during a transition, understanding the dynamics of saturation is thus essential to design an efficient training system.

1 INTRODUCTION

An important aspect of professional development is on-the-job training. For military occupations such as aircraft technicians (Bourque, 2019), this process is formalized as a progression where apprentices (mentees) receive training under the supervision of journeymen (mentors) before becoming mentors themselves. Crucial to maintaining a healthy system is the ratio of mentees to mentors: A low ratio means that there are enough mentors to train all the mentees present, and the system is in a healthy state. However, too high a ratio causes the mentor population to become taxed, potentially affecting their primary duties as well as stall the progression of the mentees, as many are unable to be trained effectively. While this scenario is usually avoided when the system already possesses healthy population sizes, such an event may occur when the system transitions between two healthy states. In practice, this saturation effect may occur for any occupation undergoing a transition with an on-the-job training component. For example, in the case of a transition to a new aircraft, the growth of the technician population able to maintain this new aircraft may be limited due to the lack of journeymen able to supervise apprentices. Because of this example and others, understanding the dynamics of the saturation effect is important.

(Bastian and Hall, 2020) gives an excellent overview of applied methods to perform military workforce planning and modelling. Given the coupled relationships present in on-the-job training scenarios and their associated complexities, discrete-event simulations are the most common method of analysing these systems (Novak et al., 2015; Zais and Zhang, 2015; Henderson and Bryce, 2019). Another common approach is to utilize industrial system dynamics (Forrester, 1965), which visualizes the continuous feedback loops, upwards flow, and interaction within these training structures (Séguin, 2015).

Lahteenmaa-Swerdlyk, T. and Bourque, F.
Investigation of Workforce Dynamical Behaviour from a Phase Plane Perspective.
DOI: 10.5220/0012270900003639

In *Proceedings of the 13th International Conference on Operations Research and Enterprise Systems (ICORES 2024)*, pages 35-46
ISBN: 978-989-758-681-1; ISSN: 2184-4372

However, these structures are often difficult to investigate due to their highly coupled nature. To alleviate these issues, differential equations (Boileau, 2012; Diener, 2018) and other statistical models (Bryce and Henderson, 2020; Okazawa, 2020) are used to investigate simplified setups to verify the system dynamics. However, this analysis is generally completed with the populations already at a healthy state as this greatly simplifies the equations which are used (Diener, 2018; Vincent and Okazawa, 2019). In practice, many key decisions must be made during transitions between healthy states and these situations must be analysed accordingly. To consider this, (Schaffel et al., 2021) utilized a set of simplified differential equations which is based on a predator-prey model (Swift, 2002). This consists of a two-state model which considers time-variable saturation effects on the training rate of mentees as the mentor population evolves. (Schaffel et al., 2021) investigated the system using a benchmark scenario and applied it to a Discrete Event Simulation. However, a deeper analysis of the governing equations are required to fully understand its system dynamics and its application to a realistic training scenario.

The aim of this paper is to analytically solve and investigate this continuous two-state population model by looking at its phase plane. The model focuses on an application to the training of aircraft technicians, which is its intended use. A benchmark scenario is first used as a backdrop to understand the system behaviour as input parameters are adjusted, before investigating its analytical solutions. Special attention is put into optimally reducing the time to reach desired healthy populations. The remainder of this paper is organized as follows. In Section 2, the system of equations governing the upgrade process is introduced, along with a benchmark scenario. Section 3 gives an overview of the system dynamics by plotting numerical solutions of the benchmark scenario. Section 4 then provides a more in-depth explanation of the observations made in Section 3 by solving the individual training regimes and investigating their various properties. The settling time is defined and investigated in Section 5. Finally, in Section 6 two mathematical proofs are completed to explain the behaviour observed in Section 5.

2 MODEL FORMULATION

In this section, the system of equations which governs the upgrading process of mentees to mentors is formally introduced. In Section 2.1, the system of differential equations governing the upgrading process is stated. In Section 2.2, a benchmark scenario is introduced to provide a base system for which we can begin the analysis.

2.1 Model Introduction

From (Schaffel et al., 2021), the system of equations to model the upgrade process is shown in Eqn. (1) and Eqn. (2). The equations take the form of a modified predator-prey model (Swift, 2002).

$$\dot{x} = a - b\min(x, ry), \tag{1}$$

$$\dot{y} = b\min(x, ry) - cy, \tag{2}$$

where x and y denote the mentee and mentor populations respectively, a is the intake rate of mentees into the system; b is the healthy upgrade rate of mentees to mentors, mentees requiring an average of 1/b time units of mentoring before being upgraded; r is the saturation limit, denoting the minimum number of mentors required to train one mentee; and c is the attrition rate of mentors. To define the variable upgrade rate of mentees, two possible regimes were considered:

1. The system is in the unsaturated training regime if the ratio of mentees to mentors is less than the saturation limit ($x < ry$), and there are enough mentors to train the entire pool of mentees in the system. Therefore, the mentees upgraded at the normal rate (bx).
2. The system is in the saturated training regime if the ratio of mentees to mentors is greater than the saturation limit ($x > ry$), and there are no longer enough mentors to train the entire pool of mentees in the system. Therefore, the progression of mentees to mentors is now limited to the number of mentors, who can either spread their training out equally among the pool of mentees, or focus their training on a specific quantity of mentees up to the value of the saturation limit. In either case, the rate mentees upgrade to mentors is now bry.

In this system, it is assumed that the attrition rate (c) may not be able to be readily changed, as mentors generally leave the system due to retirements. However, the intake (a) and upgrade rates (b), as well as the saturation limit (r), are controllable by adjusting the quantity, quality, and delivery method of the training, among other factors. Modifying these values may adjust the time required to transition between two healthy states or add additional stress to the system if the ratio of mentees to mentors becomes too high. At the steady state, the rate of change of both populations ($\dot{x}, \dot{y}$) are equal to zero in the unsaturated (healthy) regime, giving the relation:

$$a = bx_f = cy_f, \tag{3}$$

where x_f and y_f denote the number of mentees and mentors respectively in the target steady state. Since the intake, upgrade, and attrition rates are tied to the target population values, adjusting any of these parameters will move the steady state values of the mentee and mentor populations away from their intended target populations. By fixing the attrition rate, the intake and upgrade rates are calculated to reach the intended target populations.

This will leave the saturation limit as the sole independent variable, of which its effect on the system will be the primary focus of this paper. Finally, we are intrested in the case when the target mentor population is greater than the target mentee population ($y_f > x_f$). From Eqn. (3), this restriction results in the upgrade rate being greater than the attrition rate ($b > c$).

2.2 Benchmark Scenario

In the benchmark scenario, the mentee and mentor populations will undergo a growth, transitioning from an initial state (x_0, y_0) to a target steady state (x_f, y_f) where the populations are doubled. The values chosen are representative of an application to the training of aircraft technicians. Specifically, the input parameters are set to the following values:

$$(x_0, y_0) = (25, 100)$$
$$(x_f, y_f) = (50, 200)$$
$$c = 0.05$$

As discussed in Section 2.1, the intake (a) and upgrade (b) rates are calculated to reach the target populations:

$$a = cy_t = 10$$
$$b = \frac{a}{x_t} = 0.2$$

From the defined values, 10 mentees enter the system on average each time unit, and each mentee requires an average of 5 time units of training before upgrading to a mentor when the system is healthy. A mentor then stays in the system for an average of 20 time units before exiting the pool.

3 SYSTEM DYNAMICS UNDER THE BENCHMARK SCENARIO

To gain an initial understanding of the system dynamics, the system was numerically solved using the fourth-order Runge-Kutta (RK-4) method. Phase plane solutions of the benchmark scenario were plotted as the saturation limit (r), the one independent variable, was varied.

To break up the solutions to the system, we note from Eqn. (1) and Eqn. (2) that the unsaturated region is not dependent on r, so the changes in the system behaviour will only occur in the saturated region. We also note from Section 2.1 that the system will remain saturated if the mentor population is decreasing (so that x is always greater than ry). Therefore for a system to exit saturation and reach steady state in the unsaturated region, we require $\dot{y} > 0$. From inspection of Eqn. (2), this occurs when $br > c$, or $r > 0.25$ in the benchmark scenario.

Further analysis of the various solutions for the benchmark scenario are completed in the subsequent sections. In Section 3.1, system solutions that reach the target populations are investigated (when $r > 0.25$). In Section 3.2, system solutions which do not reach the target populations are investigated (when $r < 0.25$). In Section 3.3, generalizations are made of the system behaviour as r is varied.

3.1 System Solutions Which Reach the Target Populations

An arbitrary value of $r = 1/3$ is chosen in Fig. 1 to showcase the relevant system dynamics, in which there must be at least three times more mentors than mentees to prevent the system from becoming saturated. The solution trajectory and velocity vectors are plotted, as well as the initial and target populations. A dashed yellow line is added to visualize the saturation limit, which is the ratio of mentees to mentors when the system crosses into saturation. For reference, the unsaturated region is present to the left of the line, and the saturated region is present to the right. There are two asymptotes in the unsaturated regime, a vertical and diagonal asymptote, which are represented as dashed-pink lines. From the plot, the solution begins at the initial populations in the unsaturated region, crosses into the saturated region, then curls, back into the unsaturated region where it reaches steady state at the target populations. The mentee population overshoots its target population, with its largest population size occurring at the inflection point in the saturated region. The system also exits the saturated region below the diagonal asymptote in the unsaturated region; with the mentor population approaching its target population from below and does not contain an overshoot.

As r is increased, the saturation limit line becomes shallower, and the system spends less time in the saturated region. Solutions of the benchmark scenario for

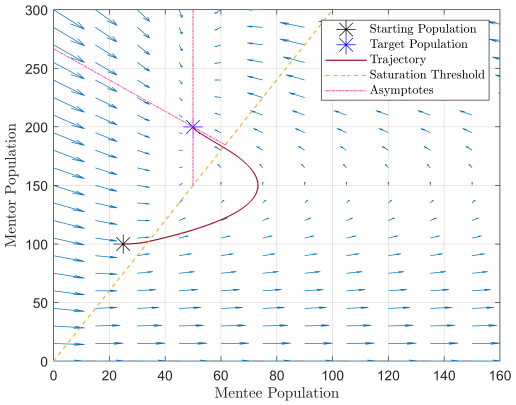

Figure 1: Phase plane of the benchmark scenario, with the saturation limit (r) set to 1/3.

increased r values are shown in Fig. 2. In Fig. 2a, r is set to 0.35, and in Fig. 2b, r is set to 0.4. Both solutions reach the steady state at the target populations. In Fig. 2a, the system has less of a mentee overshoot than the plot of $r = 1/3$ shown in Fig. 1, with the inflection point located at a smaller mentee population. In Fig. 2b, we see that the saturation limit is high enough that the system never becomes saturated. The solution does not contain an inflection point as the system is always unsaturated, with the largest mentee and mentor populations located at their target populations. In addition, since the system remains in the unsaturated region, the system no longer depends on the value of the saturation limit, so the solution remains unchanged if this value is further increased.

As r is decreased, the system spends more time in the saturated region. Solutions of the benchmark scenario for decreased saturation limit values is shown in Fig. 3. In Fig. 3a, r is set to 0.3, and in Fig. 3b, r is set to 0.28. As r is decreased, the inflection point in the saturated region occurs at a larger mentee population, as both the mentor and mentee populations experience greater overshoots from their target populations. In addition, the system takes longer to reach steady state as more time is spent in the saturated region.

3.2 System Solutions Which Do not Reach the Target Populations

Fig. 4 shows solutions for the benchmark scenario in which the system does not reach the target populations. In Fig. 4a, r is set to 0.25, and in Fig. 4b, r is set to 0.2. In Fig. 4a, the value of r is set such that the upgrade rate is equal to the attrition rate ($br = c$). As a result, the mentor population remains unchanged from its starting value while the mentee population increases to infinity. In Fig. 4b, the value of r is set

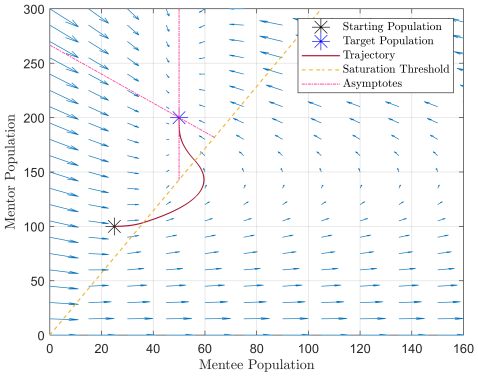

(a) $r = 0.35$.

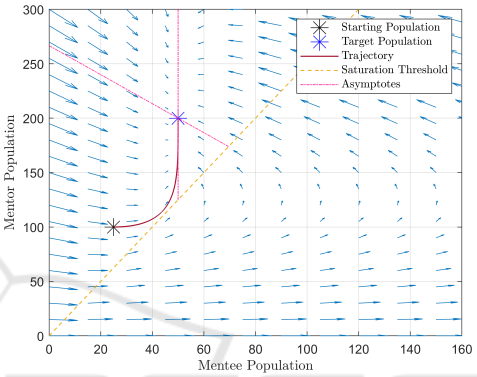

(b) $r = 0.4$.

Figure 2: Phase plane of the benchmark scenario, with the saturation limit (r) set to 0.35 (top) and 0.4 (bottom).

such that the upgrade rate is less than the attrition rate ($br < c$), in which the mentor population decreases to zero while the mentee population increases to infinity. The target populations are also located in the saturated region, so the system will never reach steady state at the target populations regardless of the initial populations.

3.3 Possible Behaviour for the System

From the phase plots in Section 3.1 and Section 3.2, we can split up the possible behaviour into three sections depending on value of the saturation limit:

- When $r \leq c/b$ ($r \leq 0.25$ for the benchmark scenario), the system remains in the saturated region and never reaches a steady state.
- When r is very high, the system reaches steady state at the target populations but always remains in the unsaturated regime.
- There exists a middle range of r values in which the system reaches the steady state at the target populations, but crosses into the saturated region for a period of time. This range is defined on the low

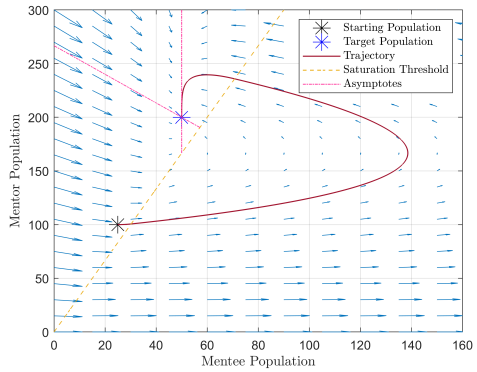

(a) $r = 0.3$.

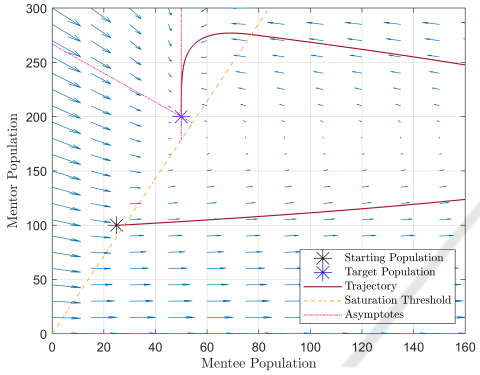

(b) $r = 0.28$.

Figure 3: Phase plane of benchmark scenario, with the saturation limit (r) set to 0.3 (top) and 0.28 (bottom).

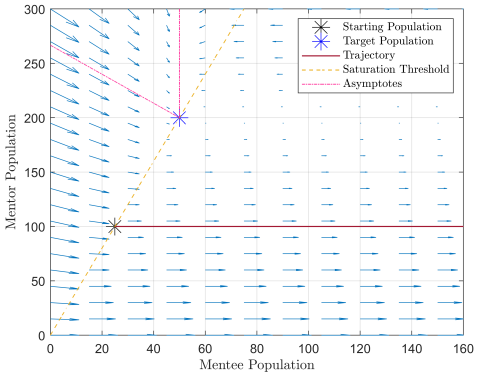

(a) $r = 0.25$.

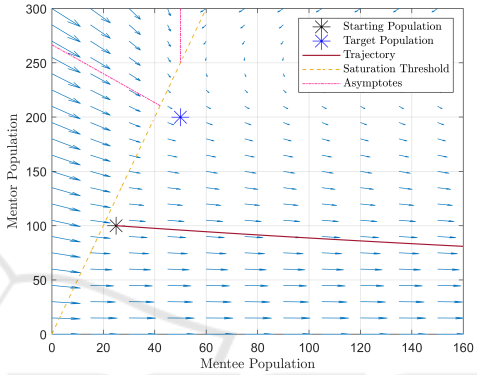

(b) $r = 0.2$.

Figure 4: Phase plane of the benchmark scenario, with the saturation limit (r) set to 0.25 (top) and 0.2 (bottom).

end by $r > c/b$ ($r > 0.25$ for the benchmark scenario), and on the high end by solving the unsaturated region equations for the r value with the solution with one intersection point with the saturation limit. For the benchmark scenario, this was found to occur when $r \approx 0.3837$, as the time in saturation was zero. Above this r value, the system never crosses into the saturated region.

We are most interested in the region of r values which reach the steady state by crossing into the saturated region ($0.25 < r < 0.3837$ for the benchmark scenario), as these solutions are dependent on more than one system of equations. The subsequent analysis contained in this paper will largely focus on this range of r values.

4 ANALYTICAL SOLUTIONS FOR AN ARBITRARY SYSTEM

From the plots of the benchmark scenario in Section 3, several important observations were made: 1.) The unsaturated region contains two asymptotes and one steady state value, 2.) The saturated region has no steady state value, and 3.) There was a range of r values in which the system reaches the target populations by crossing into the saturated region. In this case, the largest mentee population would occur at the system's inflection point in the saturated region. In this section the individual regions are further investigated by solving their respective equations for an arbitrary system. Section 4.1 and Section 4.2 provide an analysis of the unsaturated and saturated regimes respectively.

4.1 Unsaturated Region

In the unsaturated region we have the following system of equations:

$$\dot{x} = a - bx, \text{ and} \tag{4}$$

$$\dot{y} = bx - cy \tag{5}$$

This region's solution is shown in Eqn. (6) and Eqn. (7).

$$x(t) = x_f + (x_0 - x_f)\, e^{-bt} \tag{6}$$

$$y(t) = y_f + \frac{b}{c-b}(x_0 - x_f)\, e^{-bt} + \left[y_0 - \frac{b}{c-b}(x_0 - y_f) \right] e^{-ct} \tag{7}$$

The mentee (x) and mentor (y) populations decay to the target populations of x_f (a/b) and y_f (a/c) respectively as time increases, which are the target populations when the system reaches the steady state. The system approaches the target populations regardless of the initial population values (x_0 and y_0).

To determine the asymptotes in the region, we can find the angle of the system around the target population point in the phase plane, shown in Eqn. (8).

$$\tan[\theta(t)] = \frac{y(t)-y_f}{x(t)-x_f} = \frac{b}{c-b} + \frac{y_0 - \frac{b}{c-b}(x_0-y_f)}{(x_0-x_f)} e^{(b-c)t} \quad (8)$$

The asymptotes can be found by determining the initial population values which result in a constant angle (θ) for all time. From Eqn. (8), we see this is the case when either the denominator is zero, or the time-dependent exponential term is eliminated. Therefore, we can find the two asymptotes in the phase plane:

- A vertical asymptote when the initial and final mentee populations are the same ($x = x_f$).
- A diagonal asymptote with the following equation:

$$y = y_f + \frac{b}{c-b}(x-x_f) \quad (9)$$

The asymptote is at an angle centred around the target population point of $\theta = \arctan(b/(c-b))$.

From Eqn. (8), the angle of approach to the target population point is $\pm\pi/2$ as time increases to infinity since $b > c$. The only exception to this is if the trajectory is located on the diagonal asymptote. Furthermore, a solution starting above the diagonal asymptote will approach the target population point from above at an angle of $\pi/2$, containing a mentor overshoot, while a solution starting below the diagonal asymptote will approach the target population point from below at an angle of $-\pi/2$. Using these asymptotes, we can find the r value for the full solution which exits the saturated region along the diagonal asymptote. This value was numerically determined using a bisection search and finding the system with an angle of approach to the target populations which is not $\pm\pi/2$. For the benchmark scenario, this value was found to be $r \approx 0.3317$. This is analogous to a critically-damped system, as this is the smallest possible saturation limit for the benchmark scenario which prevents a mentor overshoot. The phase plane solution for this r value is shown in Fig. 5.

4.2 Saturated Region

In the saturated region we have the following system of equations:

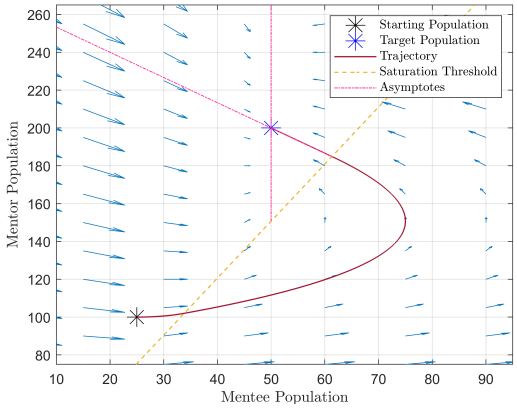

Figure 5: Phase plane of the benchmark scenario, with the saturation limit (r) set to ≈ 0.3317.

$$\dot{x} = a - bry, \text{ and} \quad (10)$$

$$\dot{y} = -\alpha y, \quad (11)$$

where $\alpha \equiv c - br$, the difference between the attrition and upgrade rates in the saturated region. This region's solution is shown in Eqn. (12) and Eqn. (13).

$$x(t) = \left(x_0 - \frac{bry_0}{\alpha}\right) + at + \left(\frac{bry_0}{\alpha}\right) e^{-\alpha t} \quad (12)$$

$$y(t) = y_0 e^{-\alpha t} \quad (13)$$

The mentee equation contains a ramp term, so the system does not have a steady state value. The behaviour of the saturated region is dependent on the value of the saturation limit, the one independent variable. If the attrition rate is greater than the upgrade rate ($c > br$), then as time increases, the mentee population approaches infinity and the mentor population decays to zero. Likewise, if the upgrade rate is greater than the attrition rate ($c < br$), then as time increases, the mentee population approaches negative infinity while the mentor population approaches infinity. Finally, if the two rates are the same ($br = c$), Eqn. (12) and Eqn. (13) simplify to Eqn. (14) and Eqn. (15). As time increases, the mentor population does not change and the mentee population goes to either positive or negative infinity at a constant rate of $a - bry_0$.

$$x(t) = x_0 + (a - bry_0)t \quad (14)$$

$$y(t) = y_0 \quad (15)$$

From Eqn. (12) and Eqn. (13), the inflection point of a system in the saturated region can be calculated by solving for when the derivative of the Eqn. (12) with respect to x is zero, given in Eqn. (16) and Eqn. (17).

$$y_{inf} = \frac{a}{br}, \quad (16)$$

$$x_{inf} = x_0 - \frac{a}{\alpha}\left[\frac{y_0}{y_{inf}} + \ln\left(\frac{y_{inf}}{y_0}\right) - 1\right], \quad (17)$$

where x_{inf} and y_{inf} denote the mentee and mentor populations respectively at the inflection point. The inflection points for the benchmark scenario are plotted in Fig. 6 for saturation limits between zero and one. The mentee population at the inflection point (x_{inf}) is shown in blue, and the mentor population at the inflection point (y_{inf}) is shown in orange. The mentor population approaches infinity at $r = 0$, and decreases to zero as r is increased. The mentee population contains two asymptotes at $r = 0$ and $r = c/b$ ($r = 0.25$ for the benchmark scenario). For low values of r, the system has an inflection point at a mentee population below zero and approaching negative infinity at the two asymptotes. For high values of r, the mentee population approaches infinity from the right at $r = c/b$, then generally decreases as r is increased. We can observe that the mentee and mentor populations at the inflection point increase as r is lowered to $r = c/b$. This will put the system deeper into saturation, putting additional stress on the mentors in the system.

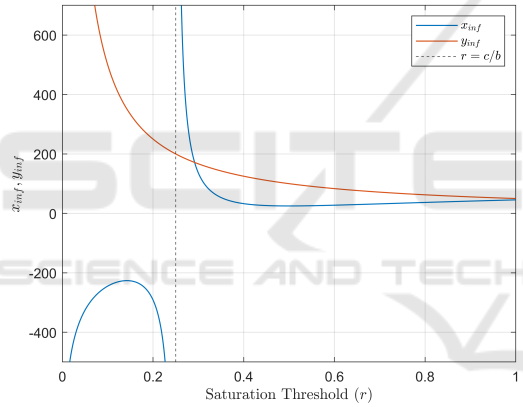

Figure 6: Mentee and mentor populations at the inflection point for the benchmark scenario as r is varied.

5 TIME TO SETTLE AT A THRESHOLD

As noted in Section 3.3, the system reaches the steady state at the target populations in the unsaturated region. In this region, the mentee and mentor populations experience an exponential decay to their steady state values, as noted in their respective equations, Eqn. (6) and Eqn. (7) shown in Section 4.1. As a result, the system approaches the target populations asymptotically, with both populations requiring a time of infinity to reach their final values. Therefore, to investigate the settling time of the system as the saturation limit (r) is varied, a settling threshold is used as a surrogate. In Section 5.1, a formal definition for the settling threshold is given. In Section 5.2, the time for the system to settle at a threshold is calculated. Finally in Section 5.3, the time to settle at a given threshold is analysed as the r is varied for the benchmark scenario.

5.1 Settling Threshold Definition

The settling threshold σ is defined radially around the target population point in the phase plane, with the value of σ defining the threshold radius. The threshold equations in the phase plane are defined by Eqn. (18) and Eqn. (19), forming a circle centred around the target population values.

$$x(\sigma) = \sigma\cos(\theta) + x_f, \text{ and} \tag{18}$$

$$y(\sigma) = \sigma\sin(\theta) + y_f, \tag{19}$$

where $\theta \in [0, 2\pi]$.

5.2 Time Components of a Solution

As noted in Section 3.3, there are three possible behaviours the system could follow: (1) If r is too low, the system remains saturated and never reaches a steady state. (2) If r is very high, the system reaches steady state at the target populations, but remains unsaturated for all time. (3) For an intermediate range of r values, the system crosses into the saturated region but still reaches steady state at the target populations. For the second case, the settling time can be determined by solving the unsaturated equations given in Section 4.1 for the time to reach the radial threshold σ. This is completed in Eqn. (20) by finding the radius of the system around the target population point. As the system is not dependent on r, Eqn. (20) can be numerically solved for the time to reach a given threshold value σ.

$$\begin{aligned}\sigma(t)^2 &= [x(t) - x_f]^2 + [y(t) - y_f]^2 \\ &= \left[(x_0 - x_f)\,e^{-bt}\right]^2 + \left\{\frac{b}{c-b}(x_0 - x_f)\,e^{-bt} \right. \\ &\quad \left. + \left[y_0 - \frac{b}{c-b}(x_0 - y_f)\right]e^{-ct}\right\}^2,\end{aligned} \tag{20}$$

where x_0 and y_0 are the starting populations. For the third case, the process of finding the settling time is stitched from three components:

- The time in the unsaturated region from the initial population to the saturation limit. This can be determined by solving for the first intersection point of the unsaturated equations, Eqn. (6) and Eqn. (7) in Section 4.1 with the saturation limit, $x = ry$. Combining these three equations yields Eqn. (21). This

equation can be numerically solved for the time to the saturation entry point.

$$0 = (ry_f - x_f) + (x_0 - x_f)\left(\frac{rb}{c-b} - 1\right)e^{-bt} + r\left[y_0 - \frac{b}{c-b}(x_0 - y_f)\right]e^{-ct}, \quad (21)$$

- The time in the saturated region between its two intersection points with the saturation limit. This can be determined similarly by utilizing the saturated equations, Eqn. (12) and Eqn. (13) in Section 4.2, for the system which starts at the saturation entry point, solving for the second intersection point with the saturation limit. The time in saturation is given by Eqn. (22).

$$t = \frac{x_s}{a}\left(\frac{b}{\alpha} - 1\right) + \frac{1}{\alpha}W_{-1}\left[\frac{x_s}{a}(\alpha - b)\,e^{\frac{x_s}{a}(\alpha - b)}\right], \quad (22)$$

  where W_k is the Lambert W Function, looking at its $k = -1$ branch, $\alpha \equiv c - br$, t is the time to the saturation exit point, and x_s is the mentee population at the saturation entry point.
- The time in the unsaturated regime from the saturation exit point at the saturation limit, to the given threshold σ. This can be determined by inverting Eqn. (20) for the time to reach σ, with x_0 and y_0 replaced as the saturation exit point coordinates.

5.3 Time to Settling Threshold for the Benchmark Scenario

Using the process defined in Section 5.2, the settling time was tabulated as r was varied for systems which cross into saturation ($0.25 < r < 0.3837$ for the benchmark scenario). This is shown in Fig. 7 for an arbitrary threshold of $\sigma = 1$. The individual times the system spends in each region are included, with the time from the initial populations to saturation shown in yellow, the time spent in saturation shown in red, and the time spent from saturation to the threshold σ shown in blue. Finally, the r value for the system which exits the saturated region along the diagonal asymptote in the unsaturated region is shown as a dashed vertical line labelled as r_{cr}, equal to $r_{cr} \approx 0.3317$ as noted in Section 4.1. From the plot, it is observed that solutions with low values of r take much longer to settle, as more time is spent in saturation. As r increases, the settling time approaches a specific value, which is the time for the system if it were always unsaturated. Finally, there exists a well which occurs solely in the unsaturated region as the system approaches the settling threshold. From the total settling time, the r value for the minimum settling time is less than r_{cr}. Therefore this solution overshoots the target mentor population before decaying to the steady state.

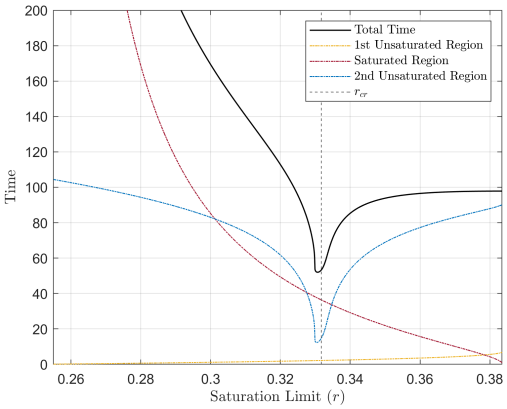

Figure 7: Total settling time to threshold and breakdown of time spent in each region for the benchmark scenario and range of interested saturation limits. The settling threshold is set to $\sigma = 1$.

The settling times for various saturation limits were analysed as the threshold σ decreased to zero. Shown in Fig. 8 are plots of the settling time for decreased threshold values of $\sigma = 10^{-1}$ in Fig. 8a, $\sigma = 10^{-3}$ in Fig. 8b, and $\sigma = 10^{-5}$ in Fig. 8c. From the plots, the time to the saturation entry point and in the saturated region remain unchanged, as they are independent of the chosen threshold. In addition, the total time to reach decreasing settling thresholds increases for all values of r, given the exponential decay to the target populations. However, the full width at half maximum (FWHM) of the well decreases in width, and the well increases in depth as the threshold goes to zero. The r value for the minimum settling time also drifts closer to r_{cr} as the threshold decreases. Therefore, the overshoot of the system with the minimum settling time decreases as the threshold goes to zero, approaching the system which exits the saturated system along the diagonal asymptote in the unsaturated region.

6 ANALYSIS OF AN ARBITRARY SYSTEM NEAR STEADY STATE

To understand the behaviour observed in Section 5.3, the interaction of the unsaturated region with the radial settling threshold is investigated by explaining two mathematical proofs. In Section 6.1, the equations for the unsaturated regime are rotated to simplify their form. Section 6.2 shows why the solution with the minimum settling time at a non-zero threshold is associated with a system overshooting the target

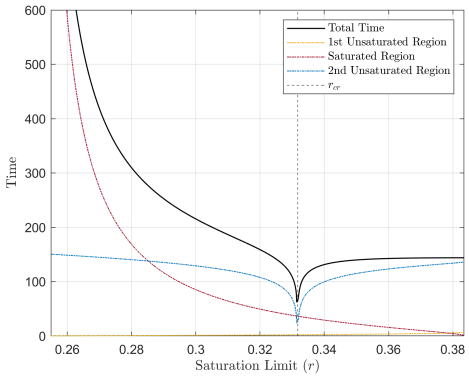

(a) $\sigma = 10^{-1}$.

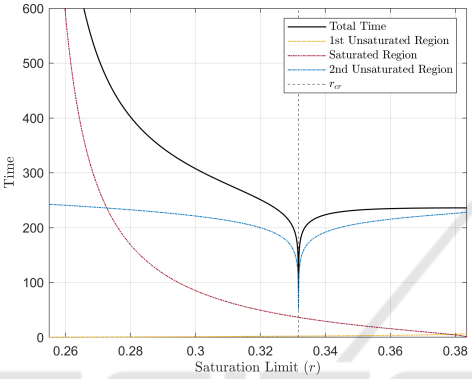

(b) $\sigma = 10^{-3}$.

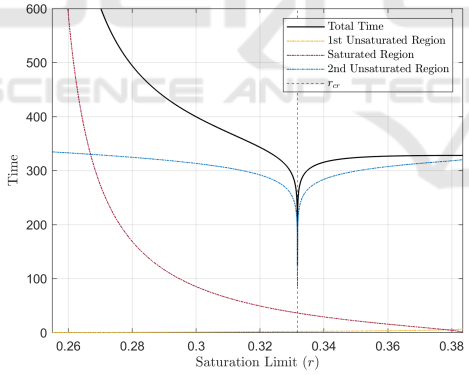

(c) $\sigma = 10^{-5}$.

Figure 8: Total settling time and breakdown of time spent in each region for the benchmark scenario and range of interested saturation limits. The settling threshold is decreased to $\sigma = 10^{-1}$, 10^{-3}, and 10^{-5}.

mentor population. Section 6.3 demonstrates that as the threshold is taken to zero, the solution along the diagonal asymptote will eventually precede all other non-diagonal solutions.

6.1 Simplification of the Unsaturated Region

To simplify the equations for the unsaturated region, the system was re-centred around the target population point and rotated such that the diagonal asymptote is present along the new x-axis. The transformed system is dubbed the $\tilde{x}(t)$ and $\tilde{y}(t)$ basis, with the $\tilde{y}(t)$ basis vector perpendicular to the $\tilde{x}(t)$-axis, the diagonal asymptote. This transformation is completed using a rotation matrix, with the angle of rotation (θ) corresponding to the angle of the diagonal asymptote in the unsaturated regime. The transformation from the $x(t)$ and $y(t)$ basis to the $\tilde{x}(t)$ and $\tilde{y}(t)$ basis is shown in Eqn. (23).

$$\begin{pmatrix} \tilde{x}(t) \\ \tilde{y}(t) \end{pmatrix} = \begin{pmatrix} \cos(\theta) & -\sin(\theta) \\ \sin(\theta) & \cos(\theta) \end{pmatrix} \begin{pmatrix} x(t) - x_f \\ y(t) - y_f \end{pmatrix}, \quad (23)$$

where $\theta = \arctan[b/(b-c)]$, noted in Section 4.1. The equations for the unsaturated regime in the $\tilde{x}(t)$ and $\tilde{y}(t)$ basis are given in Eqn. (24) and Eqn. (25).

$$\tilde{x}(t) = \tilde{x}_0 e^{-bt} + \tilde{y}_0 \left(\frac{b}{b-c} \right) \left(e^{-bt} - e^{-ct} \right), \quad (24)$$

$$\tilde{y}(t) = \tilde{y}_0 e^{-ct}, \quad (25)$$

where $\tilde{x}_0$ and $\tilde{y}_0$ denote the starting coordinates in the new basis, $\tilde{x}(0)$ and $\tilde{y}(0)$ respectively. A plot of the phase plane in the new rotated basis for the benchmark scenario is shown in Fig. 9. Note that the diagonal asymptote in the original system now becomes horizontal in the rotated system. In what follows, the "diagonal asymptote" will refer to this horizontal asymptote in the new rotated reference frame. In addition, the "vertical asymptote" will refer to the diagonal asymptote which is present.

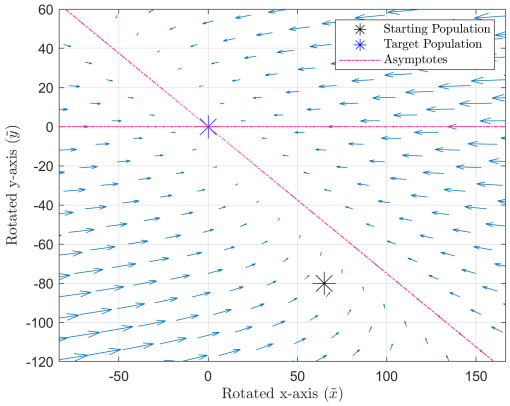

Figure 9: Phase plane of the unsaturated regime in the rotated reference frame.

6.2 Settling Time at a Non-Zero Threshold

We wish to understand why it was observed in Section 5.3 that the solution with the minimum settling time to a non-zero threshold corresponded to a system with a mentor overshoot. As noted in Section 4.1, these solutions are located above the diagonal asymptote, or $\tilde{y}(t) > 0$. In order for these solutions to reach a threshold quicker, they must travel in the phase plane at an increased velocity (i.e mentees are trained faster). From Eqn. (25), the $\tilde{y}(t)$ component of a solution is symmetrical across the diagonal asymptote ($\tilde{y} = 0$). Therefore, the difference in velocity must occur as a result of the movement in the $\tilde{x}$ direction. The velocity of solutions in the $\tilde{x}$ direction can be calculated by taking the derivative of Eqn. (24) with respect to time (t):

$$\frac{d\tilde{x}(t)}{dt} = -b\tilde{x}_0 e^{-bt} + \tilde{y}_0 \left(\frac{b}{b-c}\right)\left(ce^{-ct} - be^{-bt}\right) \tag{26}$$

The second term in Eqn. (22) has a component dependent on its distance from the diagonal asymptote ($\tilde{y}$), which is not symmetric across the asymptote. We can examine the time-dependent portion of this term, labelled as function f:

$$f(t) = ce^{-ct} - be^{-bt} \tag{27}$$

At a time of zero, the function is negative since $c < b$, while it becomes positive over time since the first term decays at a slower rate than the second term. Therefore, for positive $\tilde{y}_0$ values, the velocity at small times in the $\tilde{x}$ direction is negative but has a larger magnitude than the solutions below the diagonal asymptote. This occurs since there are more mentors present at larger $\tilde{y}_0$ values, so mentees are trained at a quicker rate. At large times, these overshooting solutions will then slow down approaching the vertical asymptote as the velocity magnitude is now smaller.

This behaviour can be observed in Fig. 10, in which several solutions starting an arbitrary distance of $\tilde{x}_0 = 100$ away are plotted and sampled at various times in Fig. 10a and Fig. 10b. At small times in Fig. 10a, the solutions above the diagonal asymptote are closer to the target population point, travelling at an increased velocity relative to solutions below the asymptote. As a result, several streamlines above the diagonal asymptote reach the plotted settling threshold of $\sigma = 10$. At large times in Fig. 10b, while all solutions decay in velocity as they approach the target population point, the solutions above the diagonal asymptote slow down and reverse direction. Only the first streamline above the diagonal reaches the smaller settling threshold of $\sigma = 1$ in around 20 time units. All other solutions have a mentor population which is too high or low to reach the threshold. By extension, as the settling threshold becomes smaller, the solution with the fastest time to the threshold must have a smaller mentor overshoot, approaching the solution along the diagonal asymptote.

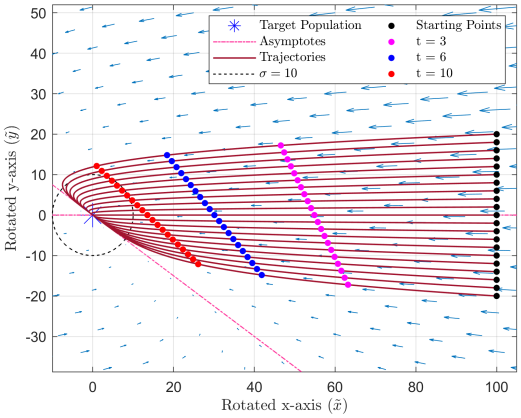

(a) Sampled at time units of 3, 6, and 10. $\sigma = 10$.

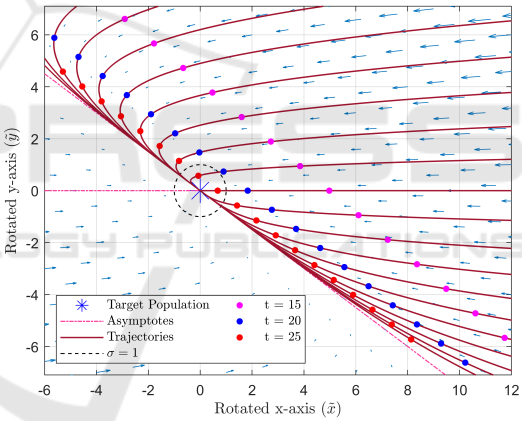

(b) Sampled at time units of 15, 20, and 25. $\sigma = 1$.

Figure 10: Plot of several solutions starting $x'_0 = 100$ away from the target population point, sampled at various times. An arbitrary settling threshold is also plotted.

6.3 Settling Time at a Threshold near Zero

We wish to understand why it was observed in Section 5.3 that the solution with the minimum settling time to a threshold approached the solution along the diagonal asymptote as the threshold was decreased to zero. While this is a logical extension to the discussion in Section 6.2, a mathematical proof for generalized input parameters is given below. In the original system, since the input parameters (a, b, c, r, x_0, y_0) can vary, a solution can approach the target popula-

tion point from anywhere in the phase plane. Therefore, we need to show that given two systems in the unsaturated regime: The first starting along the diagonal asymptote an arbitrary distance away from the target population point, and the second which can start anywhere else in the phase plane, the solution with the minimum time to reach a threshold is the solution along the asymptote, as the threshold nears zero. We will define the system along the asymptote as System 1, and the system starting anywhere else in the phase plane as System 2.

We note that if a system has the fastest time to reach a threshold, then the all other systems are further away from the target population at this time. Therefore, we can show that the radius centred around the target population from the first system is always less than the radius from the second system as time approaches infinity. The radii of the two systems relative to the target population can be calculated from Eqn. (24) and Eqn. (25), shown in Eqn. (28) and Eqn. (29). To simplify the equations, the substitutions: $\tau \equiv e^{-bt}$, and $\phi \equiv \frac{b}{b-c}$ are made. Eqn. (24) and Eqn. (25) were used to find the radii of the two systems, shown in Eqn. (28) and Eqn. (29).

$$\sigma_1(\tau)^2 = (\tilde{x_c}\tau)^2, \tag{28}$$

$$\begin{aligned}\sigma_2(\tau)^2 &= [\tilde{x}(\tau)]^2 + [\tilde{y}(\tau)]^2 \\ &= \tilde{x_0}^2\tau^2 + \tilde{y_0}\left(2\tilde{x_0}\phi\tau^2 - 2\tilde{x_0}\phi\tau^{1+\frac{c}{b}}\right) \\ &+ \tilde{y_0}^2\left[\phi^2\tau^2 - 2\phi^2\tau^{1+\frac{c}{b}} + \left(\phi^2+1\right)\tau^{\frac{2c}{b}}\right],\end{aligned} \tag{29}$$

where the starting distance from the target population along the diagonal asymptote for System 1 is labelled as $\tilde{x_c}$, and the starting coordinates for System 2 are labelled as $\tilde{x_0}$ and $\tilde{y_0}$. Each of the starting coordinates may be any real number other than zero, such that: (1) The two systems are not separated by an infinite distance, (2) System 1 is not at the target population point, and (3) Both two systems are not on the asymptote. The difference in radii can found by subtracting Eqn. (28) from Eqn. (29), shown in Eqn. (30).

$$\begin{aligned}\sigma_2(\tau)^2 - \sigma_1(\tau)^2 &= \tau^2\left(\tilde{x_0}^2 - x_c'^2\right) \\ &+ \tilde{y_0}\left(2\tilde{x_0}\phi\tau^2 - 2\tilde{x_0}\phi\tau^{1+\frac{c}{b}}\right) \\ &+ \tilde{y_0}^2\left[\phi^2\tau^2 - 2\phi^2\tau^{1+\frac{c}{b}} + \left(\phi^2+1\right)\tau^{\frac{2c}{b}}\right],\end{aligned} \tag{30}$$

Since all systems reach the steady state at a time of infinity ($\tau = 0$), taking the limit of Eqn. (30) as τ goes to zero will yield a difference of zero. Therefore, it must be shown that the difference in radii is positive for small finite valuers of $\tau = \varepsilon$, where ε is very close to zero. From Eqn. (30), replacing τ with ε and writing out our required equality yields Eqn. (31).

$$\begin{aligned}&\varepsilon^2\left(\tilde{x_0}^2 - x_c'^2\right) + \tilde{y_0}\left(2\tilde{x_0}\phi\varepsilon^2 - 2\tilde{x_0}\phi\varepsilon^{1+\frac{c}{b}}\right) \\ &+ \tilde{y_0}^2\left[\phi^2\varepsilon^2 - 2\phi^2\varepsilon^{1+\frac{c}{b}} + \left(\phi^2+1\right)\varepsilon^{\frac{2c}{b}}\right] > 0\end{aligned} \tag{31}$$

Eqn. (31) can be rearranged and divided through by ε^2 to yield Eqn. (32).

$$\begin{aligned}&\therefore \left(\tilde{x_0}^2 - x_c'^2\right) + 2\tilde{x_0}\tilde{y_0}\phi + \tilde{y_0}^2\phi^2 > \\ &\varepsilon^{\frac{c}{b}-1}\left[\left(2\tilde{x_0}\tilde{y_0}\phi + 2\tilde{y_0}^2\phi^2\right) - \varepsilon^{\frac{c}{b}-1}\left(\phi^2+1\right)\right]\end{aligned} \tag{32}$$

From Eqn. (32), the left-side can be any real, finite value. For the right-side, $\varepsilon^{\frac{c}{b}-1}$ is a negative exponential function and approaches infinity as ε goes to zero. Looking at the square-bracketed term, for a small but finite value of ε, the second term will overpower the first term. Therefore, the right-side of the equation will decrease exponentially to negative infinity. As a result, depending on the input starting coordinates, two cases exist: (1) The right-side of the equation will always be smaller than the left-side as ε is decreased, or (2) The equation may not hold for larger values of ε, but there is a value of ε in which the right-side will decrease and be less than the left-side for all smaller, but finite values of ε. In the first case, System 1 will always be ahead of System 2 for all times, while in the second case, System 1 begins behind System 2 but overtakes it at a finite value of time. In either case, System 1 will always end up closer to the target population point than System 2 as time increases, thereby satisfying the equality.

Since the equality is satisfied, a system approaching the steady state along the diagonal asymptote will be the closest system to the target population for large values of time, regardless of the starting coordinates of any other arbitrary system. Therefore, a system along the diagonal asymptote has the quickest time to a threshold which is approaching zero.

7 CONCLUSION

In this paper, a continuous model was used to investigate the workforce population dynamics of on-the-job training. Included in the model are the effects of a high mentee to mentor ratio, when the mentors can no longer train all the mentees present in the system. When this occurs, the system is described by a separate, unhealthy regime. A key parameter of interest was the saturation limit (r): the ratio of mentees to mentors above which the system becomes unhealthy (saturated). It was noted that to decrease the time for the system to reach the target populations, r must be set so that the system becomes saturated. This is to orient the system to take advantage of the increased

velocity near the diagonal asymptote. It was proven that the system with the minimum settling time at a non-zero threshold contains a mentor overshoot and will enter the saturated region; and as the threshold is decreased to zero, the system with the minimum settling time will approach the system which exits the saturated region along the diagonal asymptote. This is analogous to a critically damped system for the mentor population, in which the time to settle is optimally reduced while having no overshoot of mentors.

In a realistic training scenario for aircraft technicians, the time to train a required quota of new technicians can be reduced by allowing the system to become saturated since this maximizes the total number of mentees trained at once. However, this will require the system to become saturated and the populations to overshoot. While overshooting the target populations increases the time to a steady state, this orients the populations to take advantage of the increased training rate once the system exits saturation. If there is a personnel cap which is imposed to prevent a population overshoot, particularly for fully-trained technicians (mentors), there are fewer technicians to train the mentees and the system will take longer to reach steady state. The diagonal asymptote represents an equilibrium between maximizing the training rate and keeping the populations close to their target values. While the training rate can be increased by having more technicians, the drawback is that the number of technicians is further from the target value and the total time is increased. Finally, the scenario chosen corresponds to a growth phase where the populations are doubled. In a downsizing phase (e.g: populations are halved), the system may never enter saturation (depending on the initial ratio of mentees to mentors) since there are fewer mentees to train. In this case the system is more dependent on the attrition rate, since the target values are reached once enough mentors leave.

Moving forward with this model, time-dependent input parameters can be investigated. The constant values used for the parameters greatly restricted the system dynamics. In a realistic model these parameters could vary as the system evolves to optimally reduce the transient time and population overshoot, while still reaching the target populations at their intended values. For example, a solution with an optimally reduced time may hypothetically involve adjusting the input parameters over time to maximize the training rate while orienting the trajectory to reach the diagonal asymptote without becoming saturated.

REFERENCES

Bastian, N. D. and Hall, A. O. (2020). Military workforce planning and manpower modeling. In Scala, N. M. and Howard, J. P., editors, *Handbook of Military and Defense Operations Research*. CRC Press, 1st edition.

Boileau, M. L. A. (2012). Workforce modelling tools used by the canadian forces. pages 18–23.

Bourque, F.-A. (2019). Aircraft technician occupations: A policy review. Reference Document DRDC-RDDC-2019-D062, Defence Research and Development Canada.

Bryce, R. and Henderson, J. (2020). Workforce populations: Empirical versus markovian dynamics. In *2020 Winter Simulation Conference (WSC)*, pages 1983–1993.

Diener, R. (2018). A solvable model of hierarchical workforces employed by the canadian armed forces. *Military Operations Research*, 23:47–57.

Forrester, J. (1965). *Industrial Dynamics*. System dynamics series. Pegasus Communications.

Henderson, J. and Bryce, R. (2019). Verification methodology for discrete event simulation models of personnel in the canadian armed forces. In *2019 Winter Simulation Conference (WSC)*, pages 2479–2490.

Novak, A., Tracey, L., Nguyen, V., Johnstone, M., Le, V., and Creighton, D. (2015). Evaluation of tender solutions for aviation training using discrete event simulation and best performance criteria. In *2015 Winter Simulation Conference (WSC)*, pages 2680–2691.

Okazawa, S. (2020). Methods for estimating incidence rates and predicting incident numbers in military populations. In *2020 Winter Simulation Conference (WSC)*, pages 1994–2005.

Schaffel, S., Bourque, F.-A., and Wesolkowski, S. (2021). Modelling the mentee-mentor population dynamics: Continuous and discrete approaches. In *2021 Winter Simulation Conference (WSC)*, pages 1–10.

Séguin, R. (2015). Parsim, a simulation model of the royal canadian air force (rcaf) pilot occupation - an assessment of the pilot occupation sustainability under high student production and reduced flying rates. In *Proceedings of the 4th International Conference on Operatinal Reserach and Enterprise Systems (ICORES)*.

Swift, R. J. (2002). A stochastic predator-prey model. In *Bulletin of the Irish Mathematical Society*, number 48. Irish Mathematical Society.

Vincent, E. and Okazawa, S. (2019). Determining equilibrium staffing flows in the canadian department of national defence public servant workforce. In *2019 International Conference on Operations Research and Enterprise Systems (ICORES)*, pages 205–212.

Zais, M. and Zhang, D. (2015). A markov chain model of military personnel dynamics. *International Journal of Production Research*, 54:1–23.